

# Disentangling neurodegeneration from ageing in multiple sclerosis: the brain-predicted disease duration gap

## Supplementary Material

Supplementary Table 1. MRI acquisition protocols.

Centre	Barcelona I	Barcelona II	Basel	Bochum	Graz	Mainz	Milan	Naples I	Naples II
<b>Field strength</b>	3 Tesla	3 Tesla	3 Tesla	3 Tesla	3 Tesla	3 Tesla	3 Tesla	3 Tesla	3 Tesla
<b>Vendor</b>	Siemens	Siemens	Siemens	Philips	Siemens	Siemens	Philips	Siemens	GE
<b>Model</b>	Trio/Prisma	Trio	Skyra	Achieva	Prisma	Trio	Ingenia	Trio	Discovery
<b>Years of recruitment</b>	2016-2022	2016-2019	2017-2020	2011-2019	2021-2022	2017-2019	2017-2020	2016-2022	2019-2022
<b>Voxel dimensions (mm)</b>	1x1x1	0.94x0.94x0.94	1x1x1	1x1x1	1x1x1	1x1x1	1x1x1	0.8x0.8x0.8	1x1x1
<b>TR (ms)</b>	2300	1800	2300	10	1900	1900	7	3000	7
<b>TE (ms)</b>	3	3	2	4.6	2.7	2.5	3.2	2.4	3
<b>TI (ms)</b>	900	800	900	-	900	900	1000	1000	650
<b>FA (°)</b>	9	9	9	8	9	9	8	9	9
<b>Slices, Orientation</b>	176, sagittal	240, sagittal	192, sagittal	180, sagittal	176, sagittal	192, sagittal	204, sagittal	224, sagittal	206, sagittal

Centre	Oslo				Oxford	Prague	Rome	Siena	Verona	London I		London II
<b>Field strength</b>	3 Tesla	3 Tesla	3 Tesla	1.5 Tesla	3 Tesla	3 Tesla	1.5 Tesla	3 Tesla	3 Tesla	1.5 Tesla	3 Tesla	3 Tesla
<b>Vendor</b>	GE	GE	GE	Siemens	Siemens	Siemens	Siemens	Philips	Philips	GE	Philips	Philips
<b>Model</b>	Signa	Discovery	Signa	Avanto	Prisma	Skyra	Avanto	Achieva	Achieva	Signa	Achieva	Achieva
<b>Years of recruitment</b>	2012-2014	2015-2019	2019-2022	2012-2017	2018-2019	2012-2022	2018-2021	2017-2021	2015-2017	1999-2008	2014-2015	2014-2023
<b>Voxel dimensions (mm)</b>	1.2x0.5x0.5	1x1x1	0.8x0.8x0.8	1.2x1.25x1.25	1x1x1	1x1x1	1x1x1	1x1x1	1x1x1	1.5x1.5x0.9	1x1x1	1x1x1
<b>TR (ms)</b>	10.2	8.2	2356	2400	2040	2300	2200	10	8.2	10.9	6.8	7
<b>TE (ms)</b>	4.2	3.2	3	3.6	4.7	3	3.4	4	3.8	4.2	3.0	3.2
<b>TI (ms)</b>	450	450	950	1000	900	900	950	-	-	450	-	-
<b>FA (°)</b>	13	12	8	8	8	9	8	8	8	20	8	8
<b>Slices, Orientation</b>	124, axial	186, sagittal	240, sagittal	160, sagittal	192, sagittal	176, sagittal	176, axial	256, sagittal	180, sagittal	124, coronal	180, sagittal	176, sagittal

mm = millimetre; ms = milliseconds; TE = echo time; TR = repetition time; FA = flip angle.

**Supplementary Table 2. Models for the prediction of EDSS.** Coefficient estimates (with standard errors in parentheses) and model statistics for the linear regression analyses predicting EDSS.

	<i>Dependent variable:</i>		
	(1)	EDSS (2)	(3)
Brain-age gap	0.026** (0.005)		0.023** (0.005)
MS-age gap		0.031*** (0.010)	0.017 (0.011)
Age	13.786*** (1.656)	12.898*** (1.687)	14.483*** (1.709)
Age <sup>2</sup>	2.093 (1.337)	2.226 (1.354)	2.279* (1.340)
DD	0.023*** (0.006)	0.031*** (0.006)	0.023*** (0.006)
Sex	-0.094 (0.096)	-0.046 (0.096)	-0.100 (0.096)
Constant	1.900*** (0.091)	1.987*** (0.090)	1.912*** (0.091)
Observations	867	867	867
R <sup>2</sup>	0.187	0.171	0.189
Adjusted R <sup>2</sup>	0.182	0.166	0.184
Residual Std. Error	1.318 (df = 861)	1.331 (df = 861)	1.317 (df = 860)
F Statistic	39.531*** (df = 5; 861)	35.577*** (df = 5; 861)	33.445*** (df = 6; 860)

Note: MS = multiple sclerosis; DD = disease duration; df = degrees of freedom. \*p<0.1; \*\*p<0.05; \*\*\*p<0.01

**Supplementary Table 3. Growth models of EDSS and age and disease duration gaps in the early multiple sclerosis cohort.** EDSS, brain-age gap, disease duration gap, and MS-age gap are the dependent variables of multilevel linear models with timepoints nested within subjects and random intercept and slope of follow-up time per subject, including also the fixed effects of age, age<sup>2</sup> (to account for the non-linear effect of age), and sex. When modelling the disease duration gap, the fixed effect of disease duration was also included in the model to correct for disease duration-related bias (i.e., the underestimation of disease duration in long-standing pwMS and vice versa). Shown are the coefficient estimates (with standard errors in parentheses) and model statistics.

	<i>Dependent variable:</i>			
	<b>EDSS (1)</b>	<b>BAG (2)</b>	<b>DD gap (3)</b>	<b>MS-age gap (4)</b>
Follow-up time	0.058** (0.016)	0.472*** (0.089)	0.057 (0.046)	0.016 (0.052)
Age	6.614** (1.764)	-33.343** (13.972)	26.833*** (4.650)	-39.314*** (8.781)
Age <sup>2</sup>	2.736* (1.397)	-32.054*** (9.026)	-7.353** (3.177)	-18.157*** (5.371)
DD			-0.825*** (0.042)	
Sex	0.086 (0.127)	3.544*** (1.002)	0.540* (0.298)	1.163* (0.627)
Constant	1.153*** (0.080)	3.651*** (0.631)	2.800*** (0.209)	0.189 (0.405)
Observations	678	749	749	749
Log Likelihood	-964.876	-2,445.987	-1,578.271	-2,098.721
Akaike Inf. Crit.	1,949.751	4,911.975	3,178.543	4,217.443
Bayesian Inf. Crit.	1,994.943	4,958.162	3,229.349	4,263.630

Note: BAG = brain-age gap; DD = disease duration; MS = multiple sclerosis. \*p<0.1; \*\*p<0.05; \*\*\*p<0.01

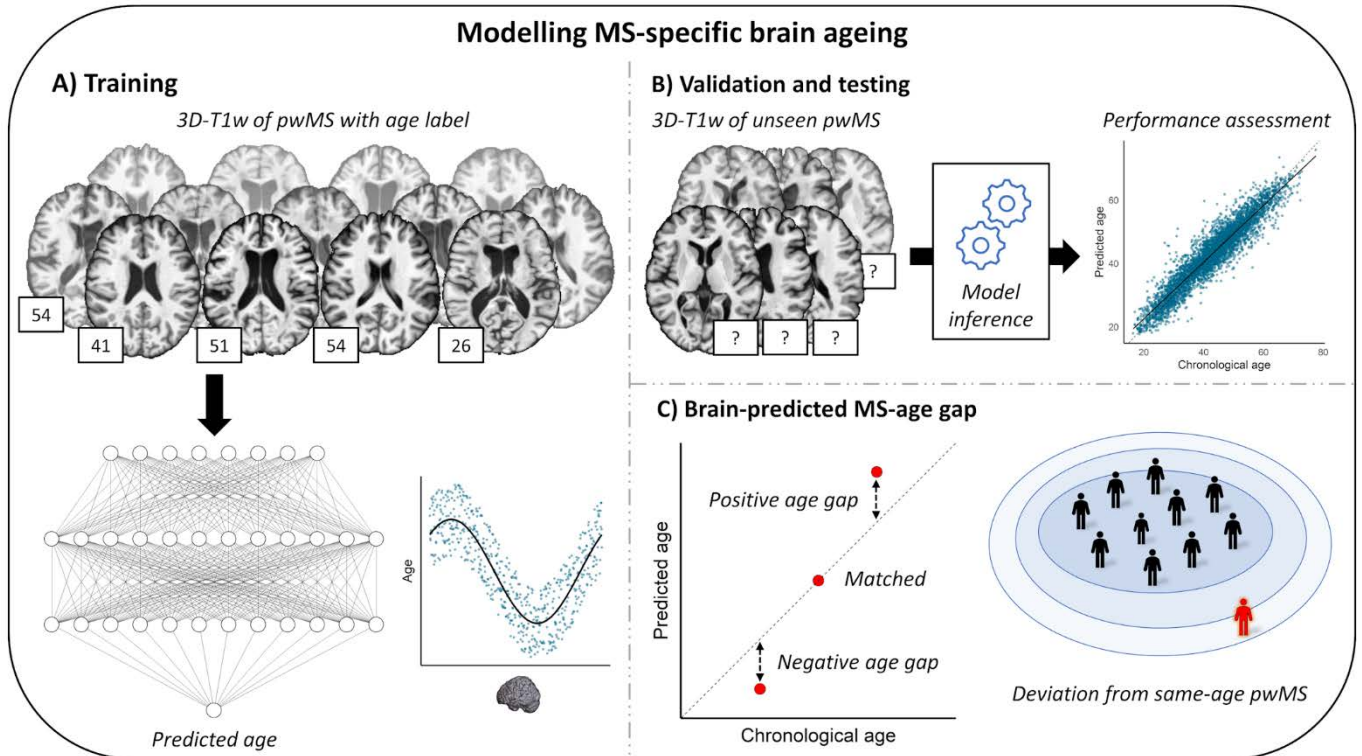
**Supplementary Table 4. Models for the prediction of annualised EDSS change.** Coefficient estimates (with standard errors in parentheses) and model statistics for the linear regression analyses predicting annualised EDSS.

	<i>Dependent variable:</i>		
		<b>EDSS annualised change</b>	
	<b>(1)</b>	<b>(2)</b>	<b>(3)</b>
Brain-age gap annualised change	0.177** (0.023)		0.193** (0.026)
MS-age gap annualised change		0.162 (0.104)	-0.152 (0.100)
Constant	-0.027** (0.012)	0.054*** (0.006)	-0.032** (0.013)
Observations	195	195	195
R <sup>2</sup>	0.228	0.012	0.238
Adjusted R <sup>2</sup>	0.224	0.007	0.230
Residual Std. Error	0.069 (df = 193)	0.078 (df = 193)	0.069 (df = 192)
F Statistic	57.158*** (df = 1; 193)	2.430 (df = 1; 193)	29.917*** (df = 2; 192)

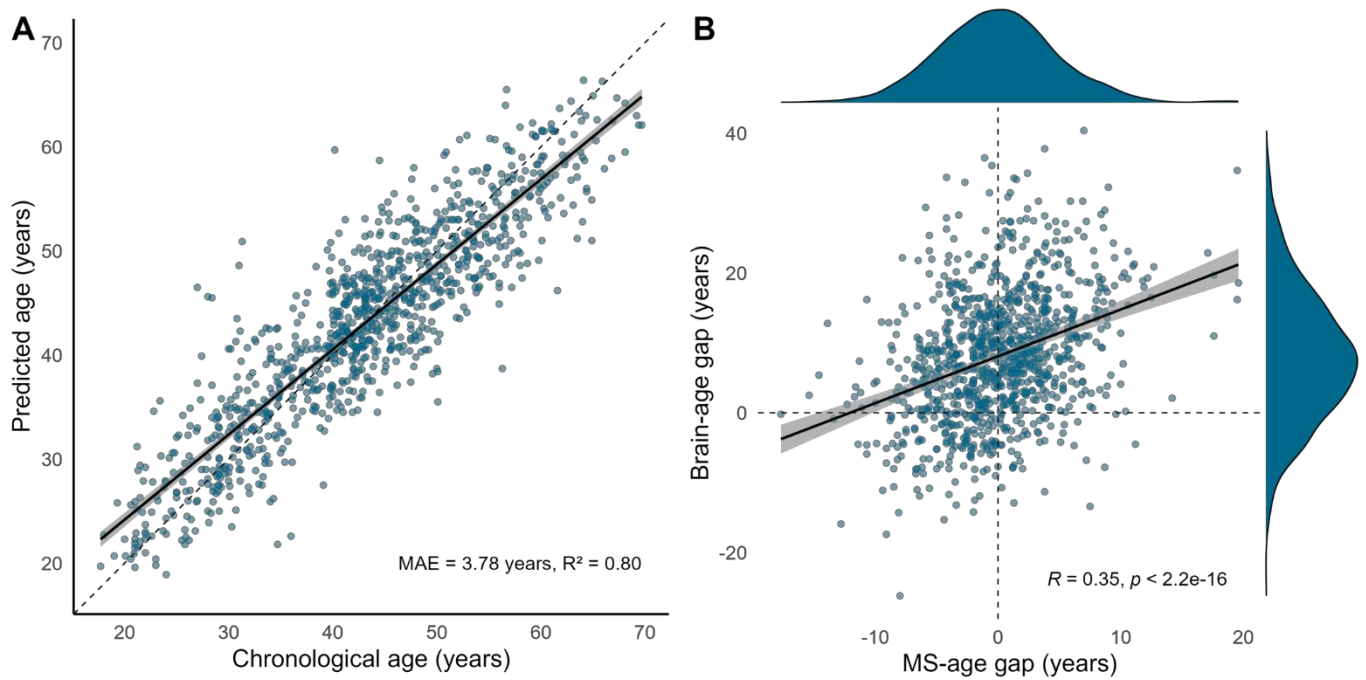
Note: MS = multiple sclerosis; df = degrees of freedom. \*p<0.1; \*\*p<0.05; \*\*\*p<0.01

### Supplementary Figure 1. Conceptual framework for the MS-age modelling strategy.

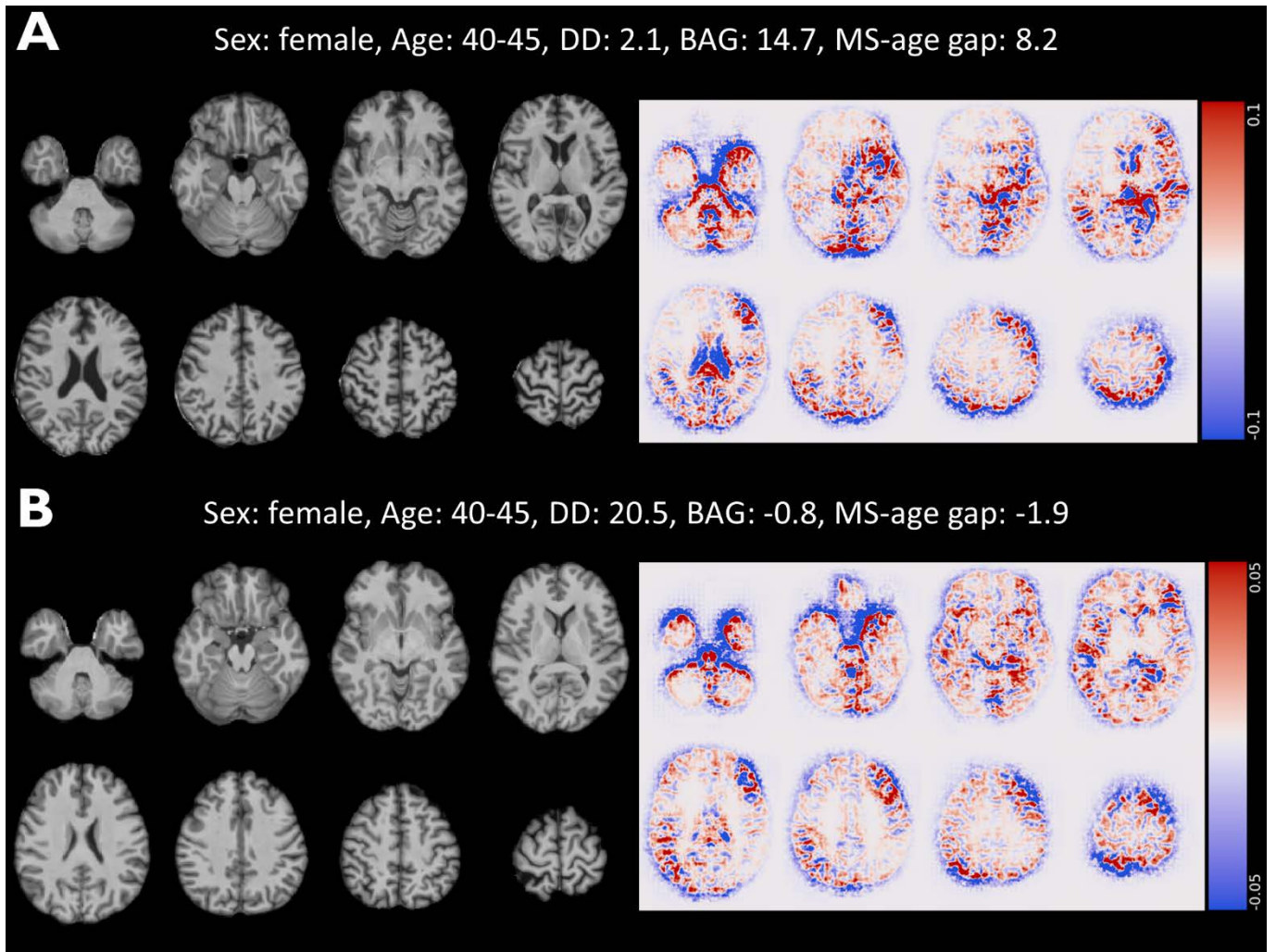
Chronological age is modelled as a function of brain MRI scans in PwMS, to estimate a reference trajectory of multiple sclerosis-specific brain ageing (MS-age). The error associated with the model predictions (the brain-predicted MS-age gap), quantifies the extent to which a patient deviates from typical multiple sclerosis-specific brain ageing.



**Supplementary Figure 2. Modelling multiple sclerosis-specific brain ageing.** In (A), scatterplot showing the relationship between chronological age in the test set ( $N = 878$ ) and the values predicted by the model of multiple sclerosis-specific ageing. In (B), scatterplot showing the relationship between the MS-age gap and the brain-age gap (obtained with the DeepBrainNet model) in the test set; marginal density plots are also shown, portraying the distribution of the two variables. Linear fit lines are shown as solid lines (with corresponding 95% confidence intervals in grey), while dashed lines represent the line of identity (A), and horizontal and vertical zero reference lines (B), respectively.



**Supplementary Figure 3. Guided backpropagation analysis to interrogate brain regions influencing the model for the prediction of MS-age.** Lightbox view of selected slices from the quasi-raw T1w volumes (on the left) and corresponding guided backpropagation-derived saliency maps (on the right) of the same subjects presented in Figure 3. For saliency maps, both positive (positively correlated with the output, in *red*) and negative (negatively correlated with the outcome, in *blue*) magnitudes are shown. In both cases, the model focuses mostly on regions that appear to be related to (the widening of) the cerebrospinal fluid spaces.



**Supplementary Figure 4. Correlations between MS-age gap and regional brain and lesion volumes.** Plots showing the correlations between MS-age gap values and cortical (A) and subcortical/lesion (B) volumes. Shown are the Pearson correlation coefficients resulting from partial correlation analyses correcting for age, age<sup>2</sup>, disease duration, sex, and estimated total intracranial volume.

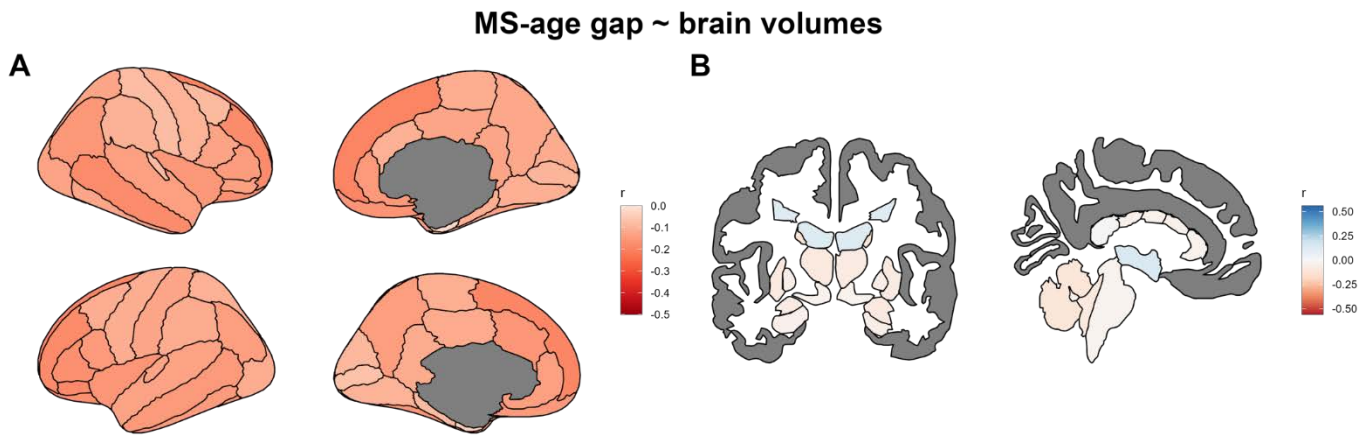
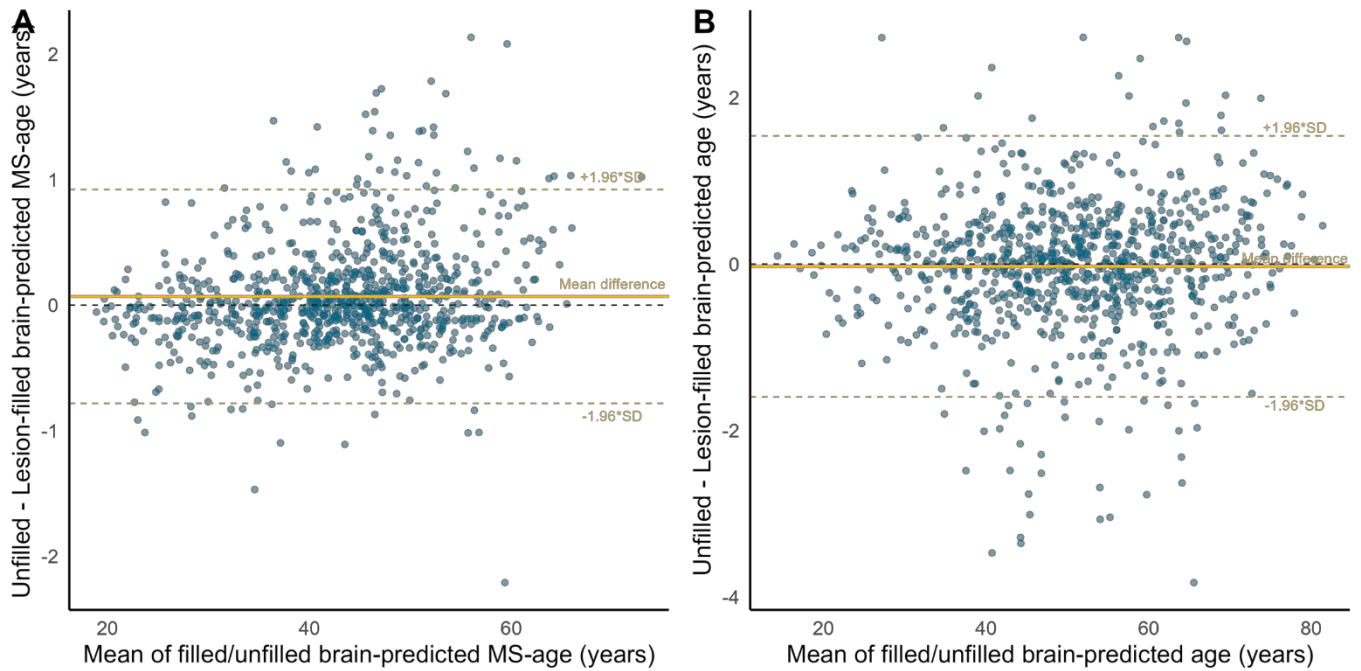
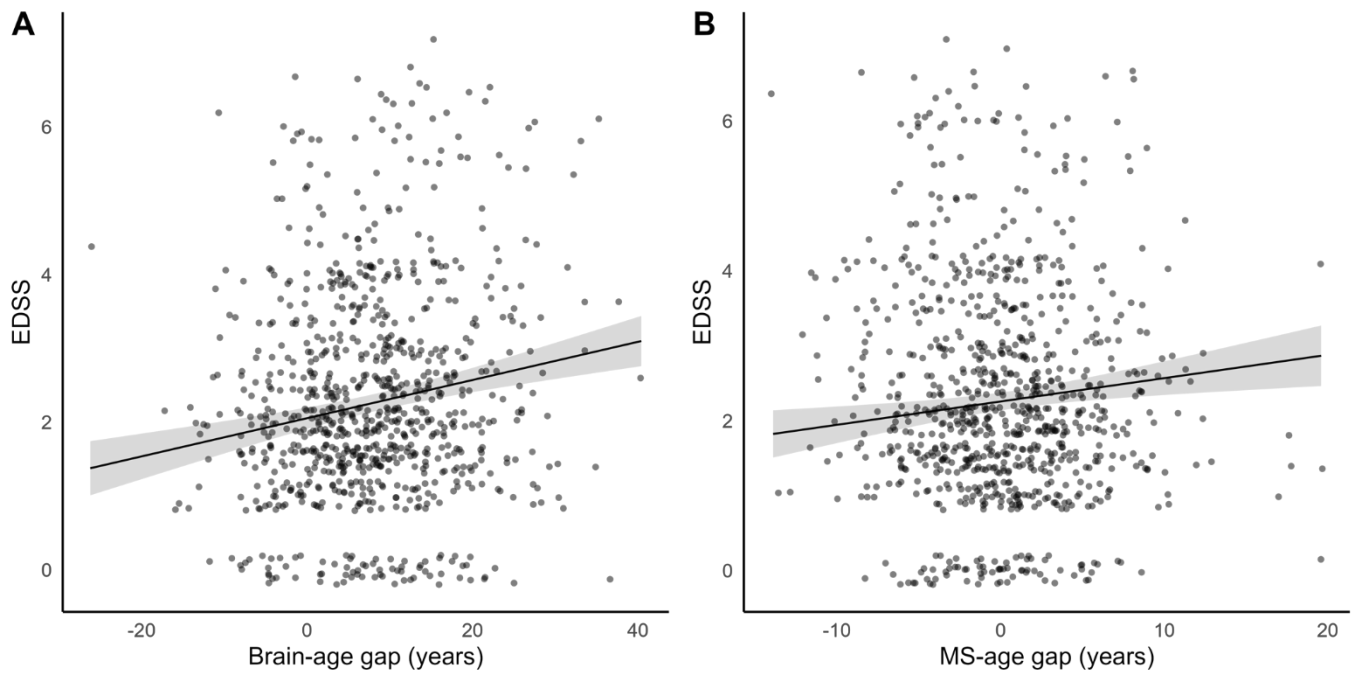




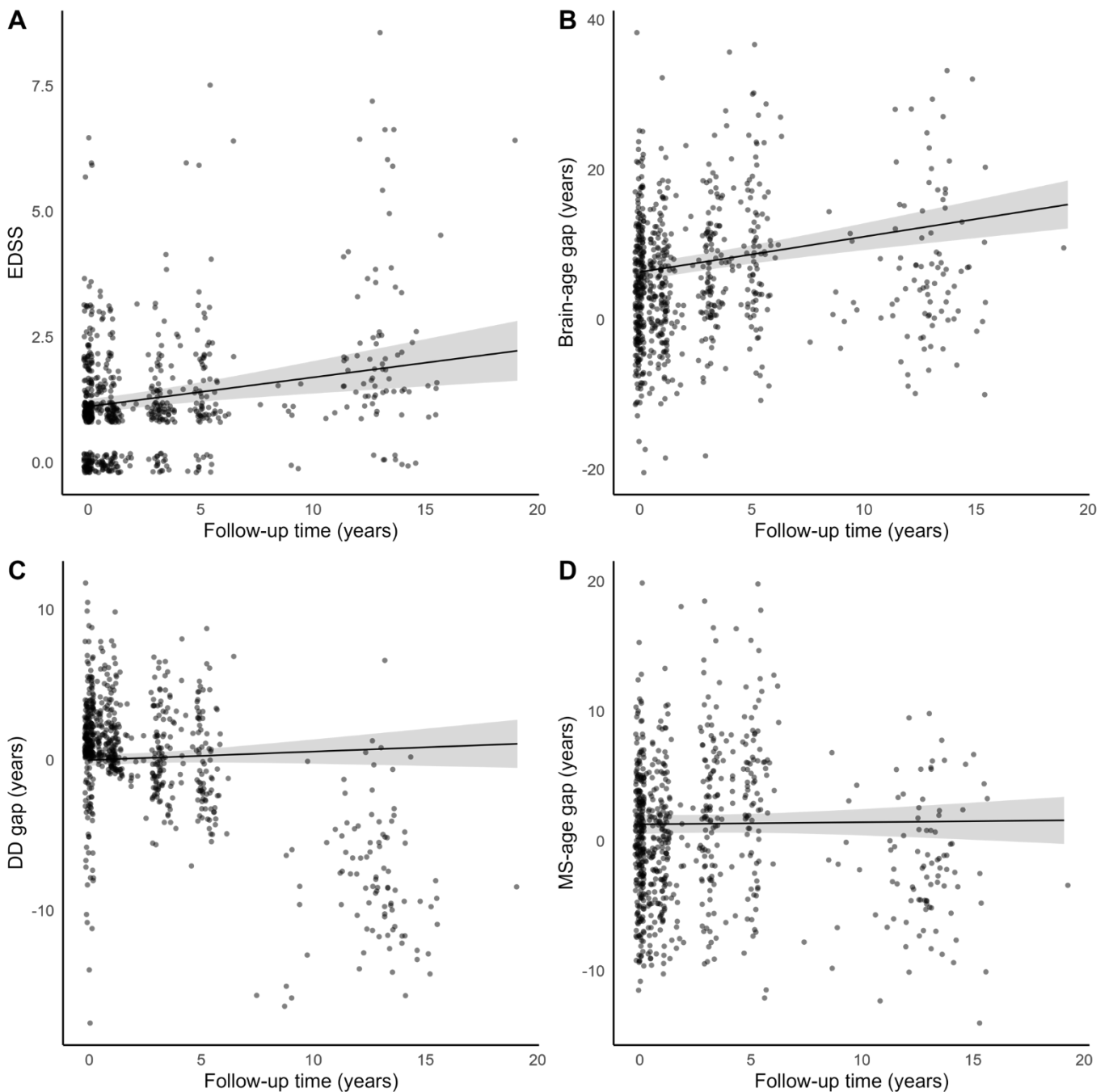
**Figure 5. Impact of MS lesions on age predictions.** Bland-Altman plot of brain-predicted MS-age (A) and age (B) from unfilled and filled T1w scans. The plots show the mean value from the 2 measures for each participant (x-axis) and the difference between the 2 measures (y-axis). The mean difference lines are solid, and the corresponding limits of agreement ( $\pm 1.96$  \* standard deviation of difference) are dashed lines.



**Supplementary Figure 6. Relationships between brain-age and MS-age gaps and physical disability.** Scatterplots showing the marginal effects on EDSS of the brain-age (A) and MS-age (B) gap metrics. Regression models were corrected for the effects of age, age<sup>2</sup>, disease duration, and sex. Linear fit lines are shown as solid lines (with corresponding 95% confidence intervals in grey).



**Supplementary Figure 7. Growth models of EDSS and age and disease duration gaps in the early multiple sclerosis cohort.** Scatterplots showing the marginal effects of follow-up time on EDSS (A), brain-age gap (B), disease duration gap (C), and MS-age gap (D). Both EDSS and brain-age gap significantly increased over time, while disease duration and MS-age gaps only exhibited a slight, non-significant, upward trend. In (C), the apparent descending trend corresponding to raw data points is to be noted, mainly reflecting the bias in the disease duration prediction model (i.e., the underestimation of disease duration in long-standing pwMS and vice versa). Linear fit lines are shown as solid lines (with corresponding 95% confidence intervals in grey).



**Supplementary Figure 8. Relationships between longitudinal changes of brain-age and MS-age gaps and physical disability.** Scatterplots showing the relationship between annualised changes of EDSS and brain-age (A) and MS-age (B) gaps. Linear fit lines are shown as solid lines (with corresponding 95% confidence intervals in grey).

